

# Synthesis of Copper(I) Oxide Thin Film Through Potentiostatic Electrodeposition as an Antioxidant Film

Muhammad Adya Raihan<sup>1,\*</sup>, Shirly Harissyah Alfiani<sup>1</sup>, Sabrina Putri Chaerani<sup>1</sup>, Rachmaniah Nurul Imani<sup>2</sup>, Alsifa Andita Putri<sup>2</sup>

<sup>1</sup>Department of Chemistry, Faculty of Mathematics and Natural Science, Universitas Negeri Jakarta, Jl. Rawamangun Muka, Jakarta 13220, Indonesia

<sup>2</sup>The Center for Science Innovation, East of Jakarta 13120, Indonesia

\*Corresponding author: madyaraihan3@gmail.com

## Received

6 September 2024

## Received in revised form

9 October 2024

## Accepted

17 October 2024

## Published online

31 October 2024

## DOI

<https://doi.org/10.56425/cma.v3i3.83>



Original content from this work may be used under the terms of the [Creative Commons Attribution 4.0 International License](https://creativecommons.org/licenses/by/4.0/).

## Abstract

Research on metal-based nanoparticles, such as silver, gold, and copper(I) oxide (Cu<sub>2</sub>O), has drawn considerable attention due to their potential applications in catalysis, antioxidants, antimicrobials, and anticancer fields. In this study, we successfully deposited Cu<sub>2</sub>O antioxidant films on indium tin oxide substrates through potentiostatic electrodeposition. The X-ray diffraction characterization revealed distinct peaks at 2θ value of 36.32°, 42.21°, and 61.30°, indicating the crystal structure of Cu<sub>2</sub>O thin film. The scanning electron microscopy image showed the three-sided pyramid morphology of Cu<sub>2</sub>O particles with average size of 316.18 nm. The energy dispersive X-ray spectrum confirmed the purity of the thin film, which is composed only of Cu and O elements without any impurities. The photoelectrochemical showed that the deposited Cu<sub>2</sub>O has a maximum photocurrent density of 8.37 mA/cm<sup>2</sup> under visible light irradiation and 1.40 mA/cm<sup>2</sup> without irradiation. In addition, this study also found that the highest inhibition values of DPPH (2,2-diphenyl-1-picrylhydrazyl) radicals were observed when ascorbic acid was added.

**Keywords:** antioxidant, ascorbic acid, Cu<sub>2</sub>O nanofilm, electrodeposition

## 1. Introduction

Free radicals are unstable atoms, molecules, or molecular fragments that undoubtedly cause oxidative stress and harm body cells. This imbalance of oxidation and reduction reactions unquestionably damages human cells and tissues, exacerbating health issues such as degenerative diseases, mutations, and premature aging. Antioxidants protect the skin, eyes, and other bodily tissues by efficiently neutralizing free radicals and lowering oxidative stress [1–4].

Researchers are increasingly interested in materials with high antioxidant content for various applications [5]. One exceptionally promising material is antioxidant film. These films are becoming more popular in biomedical applications due to their biocompatible nature and functional properties. They are used in invasive medical devices, tissue engineering substrates, drug delivery systems, antioxidants, and antimicrobial coatings [6].

These applications demonstrate the diverse role of thin films in advancing biomedical technologies and enhancing healthcare outcomes.

The antioxidant film refers to a thin layer of material, typically ranging from fractions of nanometers to micrometers in thickness, with the potential to act as an antioxidant [7]. This film can be constructed on a substrate, such as Indium Tin Oxide (ITO) and Fluorine-doped Tin Oxide [8]. It can be synthesized using various methods, including physical vapor deposition, chemical vapor deposition, electrodeposition, sol-gel, and atomic layer deposition [7,9].

Electrodeposition stands out for its ability to finely control deposition variables, such as time, temperature, frequency, potential, and pH [10–12]. Furthermore, electrodeposition features low cost, environmentally friendly, easy scale-up, good control in composition, and great flexibility in the substrate compatibility [12]. The

electrodeposition approach is beneficial for synthesizing Cu<sub>2</sub>O thin film because it allows for synthesis at room temperature and provides perfect control over the film morphology and surface characteristics [13].

Copper(I) Oxide (Cu<sub>2</sub>O) is a p-type semiconductor with a band gap of about 2 eV and is considered a potential material for electronics, solar energy conversion, and catalysis [14,15]. Currently, Cu<sub>2</sub>O have been introduced by the US Environmental Protection Agency (EPA) as effective antibacterial agents and used as drug carriers for antioxidant and antimicrobial applications [14,16]. The antioxidant capabilities of Cu<sub>2</sub>O depend on their crystal structure, chemical composition, surface charge, particle size, and surface-to-volume ratio [17]. Cu<sub>2</sub>O are reported for the treatment of cancer diseases [18], oxidative stress [19], and cardiovascular diseases [14]. Nowadays, the antioxidant potential of copper oxide nanoparticles is being intensively researched by scientists. For example, the synthesized CuO/Cu<sub>2</sub>O from the leaves of *Phoenix dactylifera* are reported to have the highest antioxidant activity at a concentration of 6 mM CuSO<sub>4</sub>.5H<sub>2</sub>O with a value of 65.1 ± 3.1 mg EAA/g (DPPH IC<sub>50</sub> = 0.386 mg/mL) [14]. Other research shows that Cu<sub>2</sub>O could enhance the antioxidant function in the body of Cu-deficient Kazakh sheep [20].

Ascorbic acid is one of the strongest antioxidants and can interact with other antioxidant candidates, such as Cu<sub>2</sub>O and Au to provide synergistic protective effects [21,22]. It also provides better control for the self-assembly of nanostructures [23]. According to Razaq et. al. [22], the antioxidant activity of gold nanoparticles (G@Glassy Carbon) increased when the concentration of ascorbic acid increased (ranging from 0.0 μM, 0.37 μM, 0.57 μM, 0.94 μM, 1.50 μM, 2.26 μM, 2.83 μM, 3.77 μM, 5.66 μM, 7.54 μM, 9.43 μM, 13.2 μM). Moreover, a sample that didn't add ascorbic acid showed the lowest DPPH (2,2-diphenyl-1-picrylhydrazyl) free radical scavenging activity. From these findings, it can be concluded that ascorbic acid could enhance the antioxidant activity of materials [22].

Therefore, this study aims to observe the potential of Cu<sub>2</sub>O acting as antioxidant film and determine the enhancement of antioxidant activity by adding ascorbic acid to Cu<sub>2</sub>O thin film. This thin film was synthesized on ITO substrate by potentiostatic electrodeposition for 60 min at a constant temperature of 50 °C, potential of -0.3 V vs Ag/AgCl, and pH of 10.

## 2. Materials and Method

### 2.1 Materials

The materials used in this research were CuSO<sub>4</sub>.5H<sub>2</sub>O (Merck), lactic acid 3.0 M (Sigma-Aldrich), ITO, Na<sub>2</sub>SO<sub>4</sub> (Merck), NaOH (Merck), 2,2-diphenyl-1-picrylhydrazyl (Sigma Aldrich) and ethanol (Merck, purity 98.0%).

### 2.2 Electrochemical deposition of Cu<sub>2</sub>O thin film

The electrodeposition of Cu<sub>2</sub>O thin films is based on previous research [24], with minor modifications. Electrodeposition was conducted using a three-electrode electrochemical cell with a platinum (Pt) wire as a counter electrode, an ITO as a working electrode, and Ag/AgCl as a reference electrode. Before deposition, the ITO substrates were treated by rinsing with ethanol and distilled water three times each to enhance the adhesion of Cu<sub>2</sub>O on the ITO surface. Subsequently, the substrate was immersed in a solution containing 0.05 M CuSO<sub>4</sub>, 3.0 M lactic acid, and 0.2 M Na<sub>2</sub>SO<sub>4</sub>. The solution was adjusted to a pH level of 10 using NaOH 10 M. The potential was set at -0.3 V vs Ag/AgCl, and the deposition time was 60 minutes. The solution temperature was maintained at 50 °C using a water bath. After the deposition, the thin film was thoroughly cleaned with distilled water and dried at room temperature [25].

### 2.3 Cu<sub>2</sub>O thin film characterization

The investigation of the Cu<sub>2</sub>O@ITO crystallography was carried out using an X-ray diffractometer (XRD, PANalytical AERIS). The resulting diffractogram is further analyzed using the X'Pert HighScore Plus application to determine the crystal structure and phase. Subsequently, scanning electron microscopy equipped with an energy-dispersive X-ray instrument was utilized to examine the surface structure, morphology, and elemental composition of the Cu<sub>2</sub>O antioxidant film.

### 2.4 Electrochemical tests

Electrochemical tests, including photoelectrochemical (PEC) and electrochemical impedance spectroscopy (EIS), were performed using a three-electrode setup. This setup included Pt as the counter electrode, Ag/AgCl as the reference electrode, and ITO as the working electrode. The PEC tests were conducted with and without solar illumination. Each test was performed in the potential range of -1.0 to 1.5 V vs Ag/AgCl at room temperature. The EIS test was conducted at the frequencies ranging from 0.1 Hz to 100 kHz.

## 2.5 Free radical- scavenging activity test

The DPPH radical scavenging assay is widely used to determine the antiradical activity of materials [26]. In this study, the ability of Cu<sub>2</sub>O thin film to scavenge DPPH radicals was measured. The Cu<sub>2</sub>O thin film was soaked in an ascorbic acid solution for 60 min, marked Cu<sub>2</sub>O-ascorbic acid. Then, Cu<sub>2</sub>O, Cu<sub>2</sub>O-ascorbic acid, and DPPH solution (as a blank) were placed into separate wells on a microplate and incubated for 210 min. Absorbance was measured every 15 min over a wavelength range of 300-500 nm.

The DPPH assay method involves observing changes in absorbance after the DPPH radical reacts with the sample. The percentage of inhibition was calculated using the following equation (1).

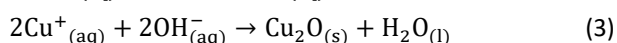
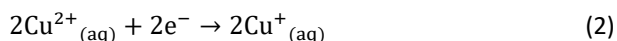
$$\% = \frac{A_0 - A_1}{A_0} \times 100\% \quad (1)$$

where % is the percentage of inhibition, A<sub>0</sub> is the initial absorbance of the DPPH solution, and A<sub>1</sub> is the absorbance of the DPPH solution after reacting with the sample.

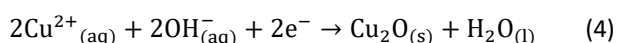
## 3. Results and Discussion

### 3.1 Mechanism for the growth of Cu<sub>2</sub>O thin film

The electrodeposition of Cu<sub>2</sub>O comprises two distinct stages. The initial stage of the process involves the reduction of Cu<sup>2+</sup> ions to Cu<sup>+</sup> ions (equation 2) and the precipitation of Cu<sup>+</sup> ions to Cu<sub>2</sub>O, which is limited by solubility (equation 3).



overall reaction:

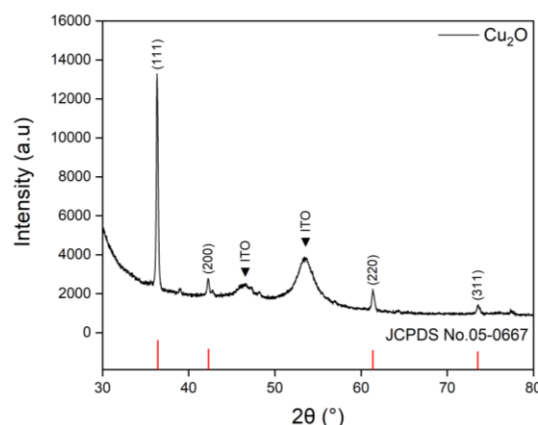


### 3.2 Morphology, composition, and structural analysis of Cu<sub>2</sub>O thin film

To determine the structural state of the Cu<sub>2</sub>O thin film, x-ray diffraction XRD was employed for characterization. The XRD characterization used a Cu-K-alpha1 radiation source ( $\lambda = 1.540598 \text{ \AA}$ ) with a potential of 40 kV and a current of 15 mA.

Based on Fig. 1 of the XRD data, the observed peaks at  $2\theta = 36.32^\circ$ ,  $42.21^\circ$ ,  $61.30^\circ$ , and  $73.46^\circ$  correspond to the crystalline planes of (111), (200), (220), and (311), respectively confirming that the thin film consists of the Cu<sub>2</sub>O cubic phase (JCPDS No. 05-0667) [35]. This finding is consistent with the research by Bandara et. al. [24], Laidoudi et. al. [25], Rahal et. al. [27], and Zhao et. al. [28],

who reported similar diffraction peaks corresponding to the crystallographic planes of (111), (200), (220), and



(311).

**Figure 1.** XRD pattern of electrodeposited Cu<sub>2</sub>O thin film on ITO substrate at a potential -0.3 V vs Ag/AgCl.

The (111) crystallographic plane is dominant in the acquired Cu<sub>2</sub>O thin film and is influenced by ITO's conductivity, which promotes a uniform electric field, favorable nucleation, and growth conditions that align with the energetically preferred (111) orientation [24]. Additionally, the XRD patterns indicate that the Cu<sub>2</sub>O thin film is of a single phase with a preferred orientation along the (111) plane.

Thin films of Cu<sub>2</sub>O that grow significantly at the (111) plane appear as three-sided pyramids or cubes, with (200) planes forming many of the lateral faces. The three-sided pyramid structure of Cu<sub>2</sub>O thin films can be attributed to the preferred crystal orientation plane at (111) [29]. Furthermore, the three-sided pyramid surface morphology of Cu<sub>2</sub>O thin film has been previously demonstrated [30].

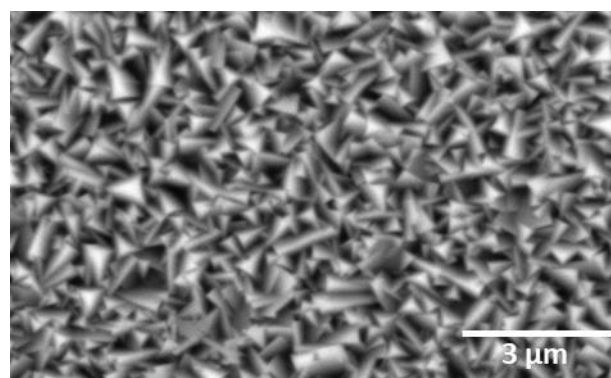


**Figure 2.** SEM image of electrodeposited Cu<sub>2</sub>O thin film on ITO substrate at a potential -0.3 V vs Ag/AgCl.

Figure 2 illustrates the surface morphology of the Cu<sub>2</sub>O thin film deposited on the ITO substrate at a potential of -0.3 V vs Ag/AgCl. As illustrated in the Fig. 2, the deposited

Cu<sub>2</sub>O exhibits a three-sided pyramidal morphology that agglomerates on the ITO surface. An analysis of the SEM image using ImageJ software revealed that the average size of the Cu<sub>2</sub>O particles is 316.18 nm, which is smaller than the result reported by Taher et. al. [31], who observed an average particle size of approximately 500 nm.

Furthermore, Fig. 2 illustrates that the Cu<sub>2</sub>O thin film exhibits a brick-red (reddish-brown) coloration. This result aligns with previous research, where the Cu<sub>2</sub>O thin film synthesized by Farhad et. al. [32] in 0.2 M CuSO<sub>4</sub> and 3 M lactic acid with a pH approximately of 9.5 and potential of -0.3 V displays a reddish-brownish color on the substrate.

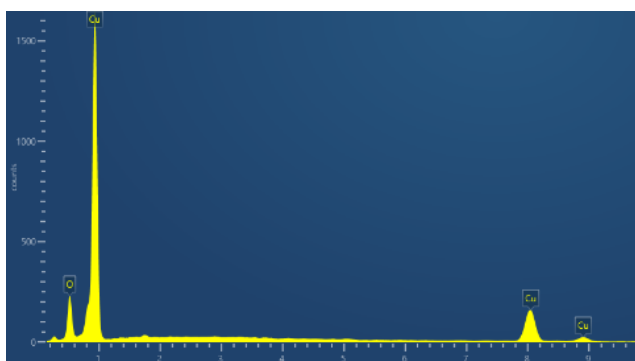


**Figure 3.** EDX spectrum of electrodeposited Cu<sub>2</sub>O thin film on ITO substrate at a potential -0.3 V vs Ag/AgCl.

The composition of the Cu<sub>2</sub>O thin film was analyzed using SEM-EDX instrument. The obtained EDX spectrum Fig. 3 confirms that the thin film contains only Cu and O elements, without any impurities. The atomic and weight ratio percentages of Cu and O elements are presented in Table 1. The deposition process on the ITO resulted in an approximate 2:1 atomic ratio of Cu to O, indicating the successful formation of the Cu<sub>2</sub>O thin film.

**Table 1.** Chemical composition of the electrodeposited Cu<sub>2</sub>O.

Element	Measurement	
	Weight%	Atomic%
Cu	89.24	67.61
O	10.76	32.39

### 3.3 Electrochemical properties

The PEC test was used to investigate the photoelectrochemical response of the electrodeposited Cu<sub>2</sub>O, providing information about the charge carriers [33]. In the PEC test, Cu<sub>2</sub>O was irradiated with visible light to trigger a photochemical reaction on the surface [34]. Figure 4 shows the relationship between the potential electrode and photocurrent density. According to the PEC results, Cu<sub>2</sub>O has a maximum photocurrent density of 8.37 mA/cm<sup>2</sup> at 0.40 V vs. Ag/AgCl under visible light irradiation

and 1.40 mA/cm<sup>2</sup> at 0.34 V vs Ag/AgCl without visible light irradiation. These findings demonstrate that Cu<sub>2</sub>O may generate significant photocurrent in a luminous environment, implying that it can absorb visible light. This result aligns with the literature, which states that all copper oxide semiconductors generate photocurrent when illuminated with visible light [34].

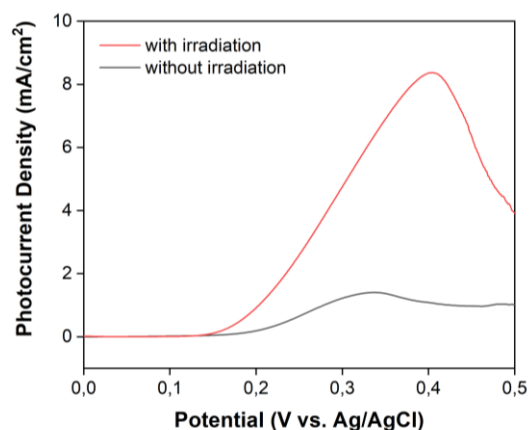
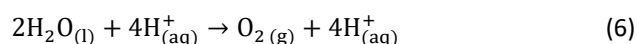


**Figure 4.** The curves of electrodeposited Cu<sub>2</sub>O thin film with and without visible light irradiation in 0.5 M Na<sub>2</sub>SO<sub>4</sub> solution.

When Cu<sub>2</sub>O was illuminated with visible light, all the open circuit potential (OCP) shifted to more positive because of the sudden creation of electron/hole pairs on the semiconductors (Cu<sub>2</sub>O). The positive shift of all the OCP reveals the p-type nature Cu<sub>2</sub>O [34]. The p-type semiconductors, like Cu<sub>2</sub>O act as photocathodes and consequently hydrogen is generated at p-type semiconductor photocathodes (equation 5) and oxygen is also generated at the counter electrode (equation 6).



EIS measurement was used to evaluate the charge transfer resistance ( $R_{\text{ct}}$ ) on the surface of the Cu<sub>2</sub>O thin film. The  $R_{\text{ct}}$  value is associated with the working electrode in the system and provides information about the resistance occurring at the Cu<sub>2</sub>O interface towards the electrolyte or its surrounding environment [35]. EIS generates a Nyquist plot, which can be used to analyze the impedance of Cu<sub>2</sub>O [25]. Figure 5 shows a Nyquist plot between a real impedance ( $Z'$ ) and an imaginary impedance ( $Z''$ ) for Cu<sub>2</sub>O thin film. The resistance of Cu<sub>2</sub>O is represented by the small half-circle of the Nyquist plot [26].

The parallel R-C curve model was employed to analyze the experimental data, which yielded an  $R_{\text{ct}}$  value of 72.42  $\Omega$  and a solution resistance value of 18.56  $\Omega$ . These findings demonstrate a superior  $R_{\text{ct}}$  compared to the study by

Athariq et. al. [36], which reported an  $R_{ct}$  of approximately 2500  $\Omega$ .

In Fig. 5, the Nyquist plot illustrates low  $R_{ct}$  values. The lower  $R_{ct}$  value indicates that the charge can be transferred more easily between the electrode and the electrolyte [26], which means high electrical conductivity.  $\text{Cu}_2\text{O}$  has semiconductor properties that actively contribute to the electron transfer process, which can accelerate the reaction mechanism. The lower resistance at the electrode surface means the charge can move faster, which makes the reaction more efficient. In conclusion, the combination of low  $R_{ct}$  values and the semiconductor nature of  $\text{Cu}_2\text{O}$  significantly influences the effectiveness of the reactions studied in this research.

The PEC test results indicate that  $\text{Cu}_2\text{O}$  thin films are efficient at transferring electrons due to their high photocurrent density, suggesting more effective electron transfer reactions [37]. In addition, the EIS test results show that  $\text{Cu}_2\text{O}$  thin films facilitate electron transfer easily as they have low  $R_{ct}$  values, contributing to improved electron transfer [38]. These findings reveal that  $\text{Cu}_2\text{O}$  thin films possess favorable electrochemical properties, enabling them to develop a charged surface.

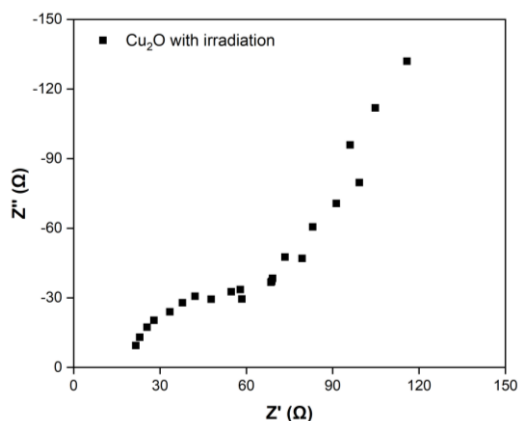


**Figure 5.** The Nyquist plot of  $\text{Cu}_2\text{O}$  thin film in 0.5 M  $\text{Na}_2\text{SO}_4$  solution under visible light irradiation.

The surface charge of  $\text{Cu}_2\text{O}$  thin films significantly impacts their antioxidant properties by directing the electrostatic interactions between the nanoparticles and the biological environment [39]. A favorable surface charge can bolster the ability of the nanoparticles to neutralize free radicals, aiding in neutralizing their reactive properties [40]. Thus, the surface charge of  $\text{Cu}_2\text{O}$  nanoparticles plays a crucial role in their antioxidant activity.

Their particle morphology can influence the electrochemical properties of  $\text{Cu}_2\text{O}$  thin films. The pyramidal shape of  $\text{Cu}_2\text{O}$  nanoparticles from this study

demonstrates better performance than the cubical shape obtained in the previous study [36]. The size of  $\text{Cu}_2\text{O}$  nanoparticles also affects their electrochemical performance [39]. Smaller particles generally exhibit a higher surface-to-volume ratio, which enhances their electrochemical reactivity by providing more active sites for electron transfer [41].

### 3.4 Antioxidant activity test

DPPH assay is a method that has been generally used as a measure to evaluate free radical scavenging activities in antioxidant analysis [26]. The principle of this method is based on the color change of the DPPH reagent. When the antioxidant compound reacts with DPPH, a proton transfer process (hydrogen atoms) occurs to stabilize the DPPH free radicals. This reaction causes the color of the system to change from purple to pale yellow. The more hydrogen atoms (H) are donated, DPPH color fades to a pale yellow [26–28].

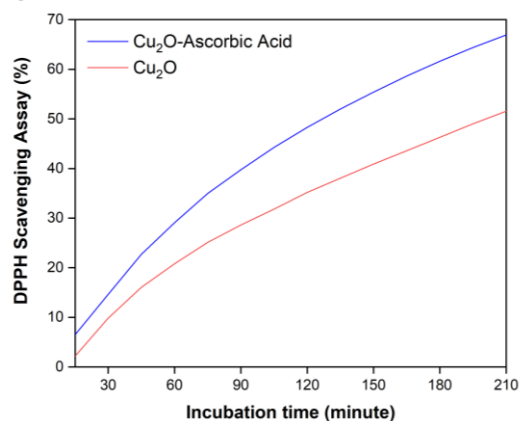


**Figure 6.** Percent inhibition as DPPH free radical scavenging activity of  $\text{Cu}_2\text{O}$  and  $\text{Cu}_2\text{O}$ -ascorbic acid.

Based on the data from Table 2 and Fig. 6, immersing the  $\text{Cu}_2\text{O}$  thin films in an ascorbic acid solution enhances its DPPH free radical scavenging activity. Furthermore, the increasing inhibition values over time indicate that the transfer of protons between  $\text{Cu}_2\text{O}$  nanoparticles and DPPH radicals is more effective with longer interaction times [3]. Figure 7 is the presumed mechanism for reducing DPPH free radicals by  $\text{Cu}_2\text{O}$  nanoparticles.

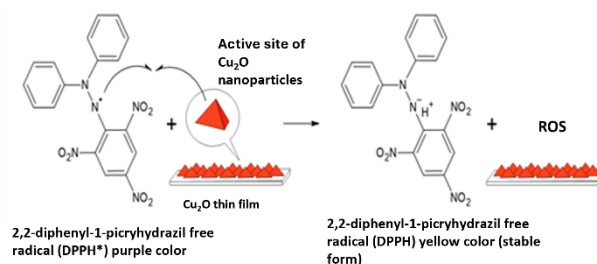


**Figure 7.** A plausible mechanism of reducing DPPH free radicals by  $\text{Cu}_2\text{O}$  nanoparticles.

From Table 2, the data show that the highest inhibition percentages were observed at 66.93% for  $\text{Cu}_2\text{O}$ -ascorbic acid and 51.55% for  $\text{Cu}_2\text{O}$  at 210 min. Moreover, the excellent antioxidant activity of the  $\text{Cu}_2\text{O}$  thin film is also influenced by its size, which is 316.18 nm or 0.316  $\mu\text{m}$ . These findings were consistent with previous literature, which states that smaller particles exhibit better antioxidant activity [42].

**Table 2.** Inhibition percentage of  $\text{Cu}_2\text{O}$ -ascorbic acid and  $\text{Cu}_2\text{O}$  after 210 minutes of incubation.

Time (minutes)	%Inhibition	
	$\text{Cu}_2\text{O}$ - ascorbic Acid	$\text{Cu}_2\text{O}$
15	6.51%	2.18%
30	14.63%	9.82%
45	22.70%	16.05%
60	29.10%	20.81%
75	34.99%	25.13%
90	39.73%	28.60%
105	44.26%	31.80%
120	48.29%	35.18%
135	51.98%	38.03%
150	55.39%	40.91%
165	58.63%	43.58%
180	61.63%	46.30%
195	64.37%	49.01%
210	66.93%	51.55%

To understand the bonding of ascorbic acid to the surface of  $\text{Cu}_2\text{O}$  after immersion, we can analyze the interactions in the process [43]. Ascorbic acid, with its hydroxyl (-OH) and carbonyl (C=O) functional groups, has the potential to interact with the  $\text{Cu}_2\text{O}$  surface through various mechanisms. It has been observed that many of the organic inhibitors, such as ascorbic acid, act by adsorption on the metal surface via negatively charged center, where its property is believed to be related to the polar groups and/or  $\pi$ -electrons [43].

The previous study, Güray Kılınççeker & Sema Çelik [43] have been reported that after immersing the electrodeposited  $\text{Cu}_2\text{O}$ - $\text{CuO}$  thin film at the ascorbic acid solution ( $1.0 \times 10^{-4}$  M), the ascorbate ions ( $\text{C}_6\text{H}_7\text{O}_6^-$ ) adsorption on the film and enhanced the protection efficiency against corrosion. Therefore, ascorbic acid is considered as an oxide phase inhibitor. Furthermore, they also mention that the chemical interaction between the metal surface of  $\text{Cu}_2\text{O}$  and the ascorbic acid followed by the removal of water molecules from the surface turns to

be chemisorptions. Four types of ascorbic acid adsorption may take place at the metal interface: (a) electrostatic attraction between charged molecules and the charged metal, (b) interaction of  $\pi$ -electrons with the metal, (c) interaction of unshared electron pairs in the molecule with the metal, and (d) a combination of the above [43].

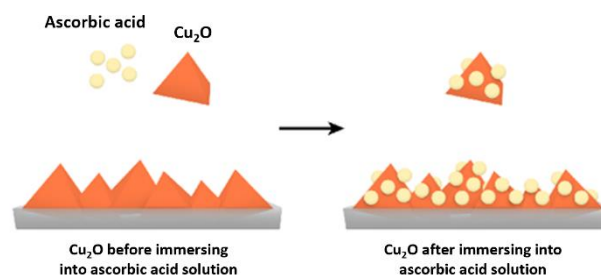


**Figure 8.** Illustration of interaction between  $\text{Cu}_2\text{O}$  nanoparticles and ascorbic acid.

The phenomenon is influenced by the nature and surface charge of the metal, the type of aggressive medium, and the chemical structure of ascorbic acid. A partial transfer of electrons from ascorbic acid directly to the vacant d orbitals present in the copper atoms can be viewed as a coordinative type of bond.

#### 4. Conclusion

The electrodeposition method successfully synthesizes  $\text{Cu}_2\text{O}$  thin films on an ITO substrate at  $50^\circ\text{C}$  under alkaline conditions, demonstrating potential applications for the preparation of antioxidant films which its antioxidant activity can be enhanced by adding ascorbic acid. The deposited  $\text{Cu}_2\text{O}$  exhibits a three-sided pyramidal morphology. In particular, the PEC test shows that  $\text{Cu}_2\text{O}$  can generate a photocurrent up to  $8.37 \text{ mA/cm}^2$  at  $0.40 \text{ V}$  under visible light irradiation. In addition, the EIS test shows the formation of Nyquist plots and the low  $R_{ct}$  of  $72.42 \Omega$ . The DPPH test shows that  $\text{Cu}_2\text{O}$ -ascorbic acid achieved 66.93% inhibition after 210 min of incubation, surpassing  $\text{Cu}_2\text{O}$ , which showed only 51.55% inhibition.

#### Acknowledgement

The authors acknowledge that this work was funded by Universitas Negeri Jakarta through KI research scheme 2023.

#### References

- [1] N.F.N.S. Fitri, A. A. Putri, R. N. Imani, S. Putriyaningsih, D. A. Sipayung, A. Sakinah, Enhancing Antioxidant Activity of Curcumin Using  $\text{ZnO}$  Nanoparticles Synthesized by Electrodeposition

- Method, *Chemistry and Materials*. **2** (2023) 77–81. <https://doi.org/10.56425/cma.v2i3.68>.
- [2] A. Sakinah, I.D. Fikri, Cocoa Powder Antioxidant Activity Test Using Cyclic Voltammetry and Differential Pulse Voltammetry Methods, *Chemistry and Materials*. **2** (2023) 30–34. <https://doi.org/10.56425/cma.v2i2.51>.
- [3] B.A. Suliasih, A. Sakinah, M. Angelina, The Effect of Electrodeposition Voltage on the Antioxidant Activity of Gold Nanoparticles, *Chemistry and Materials*. **3** (2024) 27–33. <https://doi.org/10.56425/cma.v3i1.72>.
- [4] B.A. Suliasih, D.G. Kurniawan, A. Auliya, M. Angelina, Scan rate Dependent Factor for Antioxidant Activity of Gold Nanofilms Synthesized via Cyclic Voltammetry Technique, *Chemistry and Materials*. **2** (2023) 51–55. <https://doi.org/10.56425/cma.v2i2.60>.
- [5] B. Salehi, M. Martorell, J. Arbiser, A. Sureda, N. Martins, P. Maurya, M. Sharifi-Rad, P. Kumar, J. Sharifi-Rad, Antioxidants: Positive or Negative Actors?, *Biomolecules*. **8** (2018) 124. <https://doi.org/10.3390/biom8040124>.
- [6] B.H. Billings, Thin Films, *Phys Today*. **2** (1949) 29–30. <https://doi.org/10.1063/1.3066627>.
- [7] J. Budida, K. Srinivasan, Review of thin film deposition and techniques, *Mater Today Proc*. **92** (2023) 1030–1033. <https://doi.org/10.1016/j.matpr.2023.05.004>.
- [8] R. Abdullah, N.S. Aina Arshad, Z. Zakaria, S.S. Ting, L.B. Beng, Screening of Total Phenolic Content of Antioxidant Thin Film from Pomelo (<i>Citrus grandis</i>) Peel, *Key Eng Mater*. **673** (2016) 193–202. <https://doi.org/10.4028/www.scientific.net/KEM.673.193>.
- [9] M.N. Chaudhari, Thin film Deposition Methods: A Critical Review, *Int J Res Appl Sci Eng Technol*. **9** (2021) 5215–5232. <https://doi.org/10.22214/ijraset.2021.36154>.
- [10] S. Saha, M. Johnson, F. Altayaran, Y. Wang, D. Wang, Q. Zhang, Electrodeposition Fabrication of Chalcogenide Thin Films for Photovoltaic Applications, *Electrochem*. **1** (2020) 286–321. <https://doi.org/10.3390/electrochem1030019>.
- [11] A. V. Shaikh, R.S. Mane, O.-S. Joo, S.-H. Han, H.M. Pathan, Electrochemical deposition of cadmium selenide films and their properties: a review, *Journal of Solid State Electrochemistry*. **21** (2017) 2517–2530. <https://doi.org/10.1007/s10008-017-3552-0>.
- [12] Md.A. Hossain, R. Al-Gaashani, H. Hamoudi, M.J. Al Marri, I.A. Hussein, A. Belaidi, B.A. Merzougui, F.H. Alharbi, N. Tabet, Controlled growth of Cu<sub>2</sub>O thin films by electrodeposition approach, *Mater Sci Semicond Process*. **63** (2017) 203–211. <https://doi.org/10.1016/j.mssp.2017.02.012>.
- [13] M.A. Rizqi Maulana, Aisyaturridha, Salmah Cholilah, F. Dwi Arista, Bagus Nur Listiyono, Nickel Oxide (NiO) Thin Film Synthesis via Electrodeposition for Methylene Blue Photodegradation, *Chemistry and Materials*. **2** (2023) 61–66. <https://doi.org/10.56425/cma.v2i3.62>.
- [14] B. Djamila, L.S. Eddine, B. Abderrhmane, A. Nassiba, A. Barhoum, In vitro antioxidant activities of copper mixed oxide (CuO/Cu<sub>2</sub>O) nanoparticles produced from the leaves of Phoenix dactylifera L, *Biomass Convers Biorefin*. (2022). <https://doi.org/10.1007/s13399-022-02743-3>.
- [15] M.M. Elmahdy, A. El-Shaer, Structural, optical and dielectric investigations of electrodeposited p-type Cu<sub>2</sub>O, *Journal of Materials Science: Materials in Electronics*. **30** (2019) 19894–19905. <https://doi.org/10.1007/s10854-019-02356-z>.
- [16] B. Ginting, I. Maulana, I. Karnila, Biosynthesis Copper Nanoparticles using Blumea balsamifera Leaf Extracts: Characterization of its Antioxidant and Cytotoxicity Activities, *Surfaces and Interfaces*. **21** (2020) 100799. <https://doi.org/10.1016/j.surfin.2020.100799>.
- [17] X. Zhang, K. Wang, M. Liu, X. Zhang, L. Tao, Y. Chen, Y. Wei, Polymeric AIE-based nanoprobe for biomedical applications: recent advances and perspectives, *Nanoscale*. **7** (2015) 11486–11508. <https://doi.org/10.1039/C5NR01444A>.
- [18] P. Vaid, P. Raizada, A.K. Saini, R. V. Saini, Biogenic silver, gold and copper nanoparticles - A sustainable green chemistry approach for cancer therapy, *Sustain Chem Pharm*. **16** (2020) 100247. <https://doi.org/10.1016/j.scp.2020.100247>.
- [19] M. Noman, M. Shahid, T. Ahmed, M. Tahir, T. Naqqash, S. Muhammad, F. Song, H.M.A. Abid, Z. Aslam, Green copper nanoparticles from a native Klebsiella pneumoniae strain alleviated oxidative stress impairment of wheat plants by reducing the chromium bioavailability and increasing the growth, *Ecotoxicol Environ Saf*. **192** (2020) 110303. <https://doi.org/10.1016/j.ecoenv.2020.110303>.

- [20] X. Min, Q. Yang, P. Zhou, Effects of Nano-copper Oxide on Antioxidant Function of Copper-Deficient Kazakh Sheep, *Biol Trace Elem Res.* **200** (2022) 3630–3637. <https://doi.org/10.1007/s12011-021-02975-w>.
- [21] A. Gęgotek, E. Skrzydlewska, Antioxidative and Anti-Inflammatory Activity of Ascorbic Acid, *Antioxidants.* **11** (2022) 1993. <https://doi.org/10.3390/antiox11101993>.
- [22] H. Razzaq, F. Saira, A. Yaqub, R. Qureshi, M. Mumtaz, S. Saleemi, Interaction of gold nanoparticles with free radicals and their role in enhancing the scavenging activity of ascorbic acid, *J Photochem Photobiol B.* **161** (2016) 266–272. <https://doi.org/10.1016/j.jphotobiol.2016.04.003>.
- [23] L. Vivas, I. Chi-Duran, J. Enríquez, N. Barraza, D.P. Singh, Ascorbic acid based controlled growth of various Cu and Cu<sub>2</sub>O nanostructures, *Mater Res Express.* **6** (2019) 065033. <https://doi.org/10.1088/2053-1591/ab0dd2>.
- [24] A.H.M.N.N. Bandara, V.P.S. Perera, G.K.R. Senadeera, K.N.D. Bandara, Performances of Nano-Structured Cu<sub>2</sub>O Thin Films Electrochemically Deposited on ITO Substrates in Lactate Bath as Liquid Petroleum Gas Sensors, *ECS Advances.* **2** (2023) 046501. <https://doi.org/10.1149/2754-2734/ad040a>.
- [25] S. Laidoudi, A.Y. Bioud, A. Azizi, G. Schmerber, J. Bartringer, S. Barre, A. Dinia, Growth and characterization of electrodeposited Cu<sub>2</sub>O thin films, *Semicond Sci Technol.* **28** (2013) 115005. <https://doi.org/10.1088/0268-1242/28/11/115005>.
- [26] B. Bozin, N. Mimica-Dukic, I. Samojlik, A. Goran, R. Igic, Phenolics as antioxidants in garlic (*Allium sativum* L., Alliaceae), *Food Chem.* **111** (2008) 925–929. <https://doi.org/10.1016/j.foodchem.2008.04.071>.
- [27] H. Rahal, R. Kihal, A.M. Affoune, S. Rahal, Electrodeposition and characterization of Cu<sub>2</sub>O thin films using sodium thiosulfate as an additive for photovoltaic solar cells, *Chin J Chem Eng.* **26** (2018) 421–427. <https://doi.org/10.1016/j.cjche.2017.06.023>.
- [28] W. Zhao, W. Fu, H. Yang, C. Tian, M. Li, Y. Li, L. Zhang, Y. Sui, X. Zhou, H. Chen, G. Zou, Electrodeposition of Cu<sub>2</sub>O films and their photoelectrochemical properties, *CrystEngComm.* **13** (2011) 2871. <https://doi.org/10.1039/c0ce00829j>.
- [29] Y. Yang, Y. Li, M. Pritzker, Control of Cu<sub>2</sub>O Film Morphology Using Potentiostatic Pulsed Electrodeposition, *Electrochim Acta.* **213** (2016) 225–235. <https://doi.org/10.1016/j.electacta.2016.07.116>.
- [30] K.P. Ganesan, N. Anandhan, T. Marimuthu, R. Panneerselvam, A.A. Roselin, Effect of Deposition Potential on Synthesis, Structural, Morphological and Photoconductivity Response of Cu<sub>2</sub>O Thin Films by Electrodeposition Technique, *Acta Metallurgica Sinica (English Letters).* **32** (2019) 1065–1074. <https://doi.org/10.1007/s40195-019-00876-5>.
- [31] S.J. Taher, A.A. Barzinjy, S.M. Hamad, The Effect of Deposition Time on the Properties of Cu<sub>2</sub>O Nanocubes Using an Electrochemical Deposition Method, *J Electron Mater.* **49** (2020) 7532–7540. <https://doi.org/10.1007/s11664-020-08495-y>.
- [32] S.F.U. Farhad, M.M. Hossain, N.I. Tanvir, S. Islam, Texture and Bandgap Tuning of Phase Pure Cu<sub>2</sub>O Thin Films Grown By a Simple Potentiostatic Electrodeposition Technique, *ECS Meeting Abstracts.* **MA2020-01** (2020) 1212–1212. <https://doi.org/10.1149/MA2020-01191212mtgabs>.
- [33] A. Ait Hssi, L. Atourki, N. Labchir, M. Ouafi, K. Abouabassi, A. Elfanaoui, A. Ihlal, S. Benmokhtar, K. Bouabid, High-quality Cu<sub>2</sub>O thin films via electrochemical synthesis under a variable applied potential, *Journal of Materials Science: Materials in Electronics.* **31** (2020) 4237–4244. <https://doi.org/10.1007/s10854-020-02976-w>.
- [34] M. Balik, V. Bulut, I.Y. Erdogan, Optical, structural and phase transition properties of Cu<sub>2</sub>O, CuO and Cu<sub>2</sub>O/CuO: Their photoelectrochemical sensor applications, *Int J Hydrogen Energy.* **44** (2019) 18744–18755. <https://doi.org/10.1016/j.ijhydene.2018.08.159>.
- [35] N. Ikani, J.H. Pu, K. Cooke, Analytical modelling and electrochemical impedance spectroscopy (EIS) to evaluate influence of corrosion product on solution resistance, *Powder Technol.* **433** (2024) 119252. <https://doi.org/10.1016/j.powtec.2023.119252>.
- [36] Muhamad Athariq, Muhammad Raihan Rauf, Ikhfa Wiqoy Khairany, Intan Fadia Adani, Mega Gladiani Sutrisno, Synthesis and Characterization of Nanocube Cu<sub>2</sub>O Thin Film at Room Temperature for Methylene Blue Photodegradation Application, *Chemistry and Materials.* **2** (2023) 67–71. <https://doi.org/10.56425/cma.v2i3.65>.
- [37] W. Song-Can, T. Feng-Qiu, W. Lian-Zhou, Visible Light Responsive Metal Oxide Photoanodes for Photoelectrochemical Water Splitting: a Comprehensive Review on Rational Materials Design, *Journal of Inorganic Materials.* **33** (2018) 173. <https://doi.org/10.15541/jim20170352>.



- [38] H.S. Magar, R.Y.A. Hassan, A. Mulchandani, Electrochemical Impedance Spectroscopy (EIS): Principles, Construction, and Biosensing Applications, *Sensors*. **21** (2021) 6578. <https://doi.org/10.3390/s21196578>.
- [39] L. Dou, X. Zhang, M.M. Zangeneh, Y. Zhang, Efficient biogenesis of Cu<sub>2</sub>O nanoparticles using extract of *Camellia sinensis* leaf: Evaluation of catalytic, cytotoxicity, antioxidant, and anti-human ovarian cancer properties, *Bioorg Chem*. **106** (2021) 104468. <https://doi.org/10.1016/j.bioorg.2020.104468>.
- [40] D.H. Jo, J.H. Kim, T.G. Lee, J.H. Kim, Size, surface charge, and shape determine therapeutic effects of nanoparticles on brain and retinal diseases, *Nanomedicine*. **11** (2015) 1603–1611. <https://doi.org/10.1016/j.nano.2015.04.015>.
- [41] W. Ho, Q. Tay, H. Qi, Z. Huang, J. Li, Z. Chen, Photocatalytic and Adsorption Performances of Faceted Cuprous Oxide (Cu<sub>2</sub>O) Particles for the Removal of Methyl Orange (MO) from Aqueous Media, *Molecules*. **22** (2017) 677. <https://doi.org/10.3390/molecules22040677>.
- [42] E.S. Prasedya, A. Frediansyah, N.W.R. Martyasari, B.K. Ilhami, A.S. Abidin, H. Padmi, Fahrurrozi, A.B. Juansilfero, S. Widyastuti, A.L. Sunarwidhi, Effect of particle size on phytochemical composition and antioxidant properties of *Sargassum cristaefolium* ethanol extract, *Sci Rep*. **11** (2021) 17876. <https://doi.org/10.1038/s41598-021-95769-y>.
- [43] G. Kılınççeker, S. Çelik, Electrochemical adsorption properties and inhibition of copper corrosion in chloride solutions by ascorbic acid: experimental and theoretical investigation, *Ionics (Kiel)*. **19** (2013) 1655–1662. <https://doi.org/10.1007/s11581-013-0902-5>.